ADVANCES IN ATMOSPHERIC SCIENCES, VOL. 25, NO. 4, 2008, 555–562

Impacts of Upper Tropospheric Cooling upon the Late Spring Drought in East Asia Simulated by a Regional Climate Model

XIN Xiaoge[1,2,4] (辛晓歌), Zhaoxin LI[*3,4], YU Rucong[5] (宇如聪), and ZHOU Tianjun[1] (周天军)

[1] *State Key Laboratory of Numerical Modeling for Atmospheric Sciences and Geophysical Fluid Dynamics, Institute of Atmospheric Physics, Chinese Academy of Sciences, Beijing* 100029

[2] *Graduate University of Chinese Academy of Sciences, Beijing* 100049

[3] *Laboratoire de Météorologie Dynamique, IPSL/CNRS, Université Pierre et Marie Curie, Paris, France*

[4] *National Climate Center, China Meteorological Administration, Beijing* 100081

[5] *State Key Laboratory of Severe Weather, Chinese Academy of Meteorological Sciences, China Meteorological Administration, Beijing* 100081

(Received 30 April 2007; revised 18 October 2007)

ABSTRACT

Responses of late spring (21 April–20 May) rainfall to the upper tropospheric cooling over East Asia are investigated with a regional climate model based on Laboratoire de Météorologie Dynamique Zoom (LMDZ4-RCM). A control experiment is performed with two runs driven by the mean ERA-40 data during 1958–1977 and 1981–2000, respectively. The model reproduces the major decadal-scale circulation changes in late spring over East Asia, including a cooling in the upper troposphere and an anomalous meridional cell. Accordingly, the precipitation decrease is also captured in the southeast of the upper-level cooling region. To quantify the role of the upper-level cooling in the drought mechanism, a sensitivity experiment is further conducted with the cooling imposed in the upper troposphere. It is demonstrated that the upper-level cooling can generate the anomalous meridional cell and consequently the drought to the southeast of the cooling center. Therefore, upper tropospheric cooling should have played a dominant role in the observed late spring drought over Southeast China in recent decades.

Key words: Southeast China, spring drought, inter-decadal variability, regional climate modeling

DOI: 10.1007/s00376-008-0555-x

1. Introduction

In spring (March–May), the East Asian front brings abundant precipitation to Southeast China which accounts for about 35% of the annual total amount, almost as high as that in summer (Yang and Lau, 2004). During the last half century, however, the spring precipitation over Southeast China experienced an inter-decadal decrease in the late 1970s (Hu et al., 2003; Yang and Lau, 2004; Zhai et al., 2005; Xin et al., 2006). Possible causes of this phenomenon have been mentioned in several studies. Yang and Lau (2004) showed that it is related to the basin-wide warming of the sea surface temperature (SST) in the Indian and Pacific Oceans. Xin et al. (2006) explored the atmospheric circulation changes associated with the inter-decadal drought occurred in late spring (21 April–20 May), and found that it concurs with a pronounced cooling in the upper troposphere over East Asia. They hypothesized that the upper-level cooling

*Corresponding author: Zhaoxin LI, li@lmd.jussieu.fr

induces anomalous subsidence and a low-level anticyclone, which finally led to the drought in Southeast China. The importance of an upper tropospheric thermal anomaly in explaining the observed precipitation trend in China was already pointed out in Yu et al. (2004), who studied the notable "southern flood and northern drought" trend in summer. However, the above-mentioned two studies are both based on the analysis of observation data. The causal relationship between the cooling anomaly in the upper troposphere and the change of the precipitation in East Asia needs further verification. One of the most powerful tools in this regard is numerical modeling.

As an extension study of Xin et al. (2006), this paper aims to quantify the physical mechanism linking the late spring drought and the upper tropospheric cooling over East Asia through a series of numerical simulations performed with a regionally-oriented climate model. As in Xin et al. (2006), we will use the difference between two periods of 1981–2000 and 1958–1977 to represent the inter-decadal change during the past half century. The mean atmospheric circulation data of each period will be used separately, as boundary conditions, in a regional climate model. Results are consistent with our initial hypothesis that the late spring drought in Southeast China is largely determined by the inter-decadal variation of the large-scale atmospheric circulation in East Asia. A sensitivity experiment will be further performed to quantify the role of the upper tropospheric cooling in the drought.

The other parts of this paper are organized as follows. Model description and basic performances of the model are described in section 2. Section 3 presents the simulated results about the mechanism of the late spring drought. Highlights of the findings are summarized in section 4.

2. Model description and basic performance

2.1 *Model description*

The Laboratoire de Météorologie Dynamique Zoom (LMDZ) model is a general circulation model developed at LMD (Sadourny and Laval, 1984; Le Treut et al., 1994; Li, 1999). A special feature of the model is that the model grid is stretchable in both longitude and latitude. Thus the model can be zoomed over a certain region and used for regional climate studies (Krinner and Genthon, 1998; Menendez et al., 2001; Genthon et al., 2002; Zhou and Li, 2002). With the circulation outside the zoom domain nudged to the meteorological reanalysis data, the LMDZ model can perform as a regional climate model (RCM). In this study, the RCM developed from LMDZ version 4.0 is used, hereafter referred to as LMDZ4-RCM.

The model LMDZ4-RCM used here incorporates the same physics configuration as LMDZ4, which was described in Hourdin et al. (2006) and performed in the coupled model IPSL-CM4 participating in the Fourth Assessment Report of the Intergovernmental Panel on Climate Change (IPCC, 2007). The radiation scheme is the modified version of the European Center for Medium-Range Weather Forecasts (ECMWF) scheme (Fouquart and Bonnel, 1980; Morcrette et al., 1986). The cumulus convection is parameterized with Emanuel's scheme (Emanuel, 1993). The land surface process is represented by ORCHIDEE surface-vegetation model (de Rosnay et al., 2002; Krinner et al., 2005).

In this study, LMDZ4-RCM is run with 120 points in longitude, and 91 points in latitude. The distribution of model grids over East Asia as well as the model topography is represented in Fig. 1. The zoom domain is centered at (32°N, 102°E) covering almost all of China with the horizontal resolution about 60 km. There are 19 hybrid layers in the vertical with 4 layers above 20 km. The 40-yr reanalysis data of the European Centre for Medium-Range Weather Forecasts (ERA-40, Uppala et al., 2005) are used to drive the circulation outside the zoom region. The driving variables include the zonal wind, meridional wind, temperature, and specific humidity. In all the experiments, the model is forced by the SST and sea ice cover varying with a climatologically annual cycle.

2.2 *Basic performance*

To increase our confidence in the RCM simulation, LMDZ4-RCM is firstly integrated from 1 March to 31 May in each year during the period 1990–1999. After

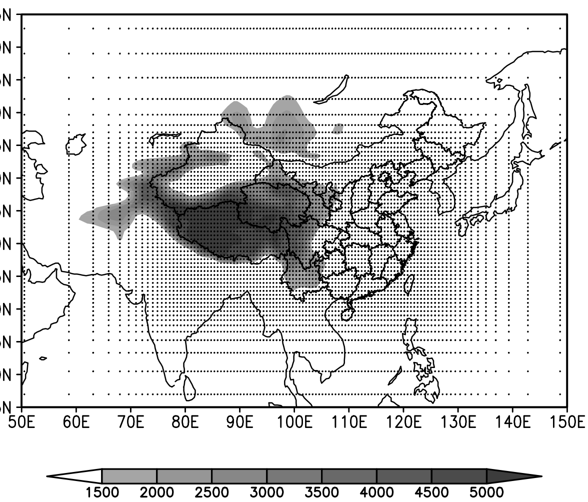

Fig. 1. Schematic representation of the model grids with zoom center at (32°N, 102°E). The shaded denotes the model topography above 1500 m.

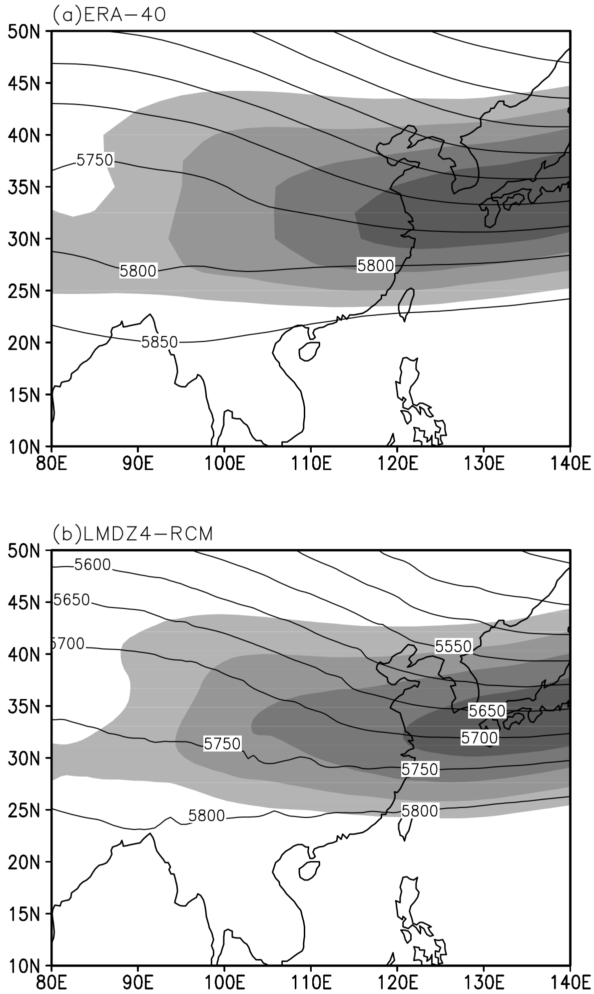

Fig. 2. April–May (AM) mean 200-hPa zonal wind (shaded, m s^{-1}) and 500-hPa geopotential height (contour, gpm) (a) revealed by ERA-40 and (b) simulated by LMDZ4-RCM averaged during 1990–1999.

a spin-up of one month, the output averaged during April and May (AM) can be regarded as the model's equilibrium result. The simulated 10-yr mean climate conditions in AM are validated against the ERA-40 circulation data and the station observed precipitation data. The precipitation dataset covers 326 stations in East China, which are provided by the National Meteorological Information Center and the China Meteorological Administration.

The upper-level jet stream and the East Asian trough are major circulation systems over East Asia. Figure 2 compares the 1990–1999 averaged AM-mean 200-hPa zonal wind (shaded) and 500-hPa geopotential height (contour) between ERA-40 and the simulation. In ERA-40, the jet stream at 200 hPa extends from East Asia to the North Pacific Ocean, with the jet core at about 32°N (Fig. 2a). East China is located in the entrance area of the jet stream. As shown in Fig. 2b, the LMDZ4-RCM model produces similar characteristics and structure. At 500 hPa, the East Asian trough dominates over East Asia with the northwesterly prevailing over East China (Fig. 2a). This is also well reproduced by the model, although the simulated geopotential height is a little weaker than that in ERA-40 (Fig. 2b).

Figure 3 shows the observed and simulated 10-yr mean precipitation (shaded) and 850-hPa meridional wind (contour) in AM. The observation exhibits abundant rainfall in Southeast China associated with strong low-level southerlies. The rainfall decreases gradually from south to north in East China. Such distribution of the precipitation is well reproduced by the model with, however, some discrepancies in intensity. Temporal (pentad mean) evolutions of precipitation along the longitudes of 107°–122°E are plotted in Fig. 4. Consistent with the observation, the simulation exhibits heavy precipitation in southeastern China during Pentad (P) P25 and P28–30. In North China

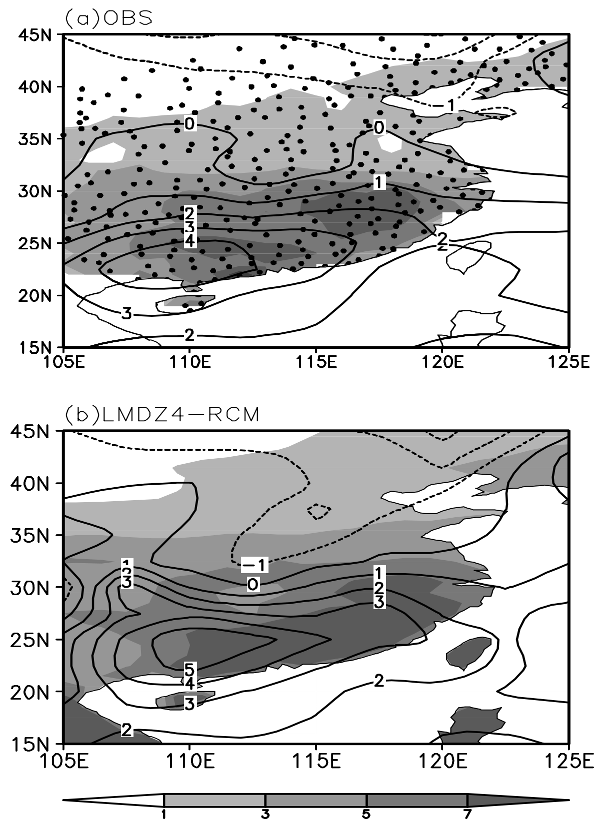

Fig. 3. AM mean precipitation (shaded, mm d^{-1}) and 850-hPa meridional wind (contour, m s^{-1}) (a) depicted by ERA-40 and (b) simulated by LMDZ4-RCM averaged during 1990–1999. Dots in (a) indicate geographic locations of the meteorological station entering into the precipitation dataset.

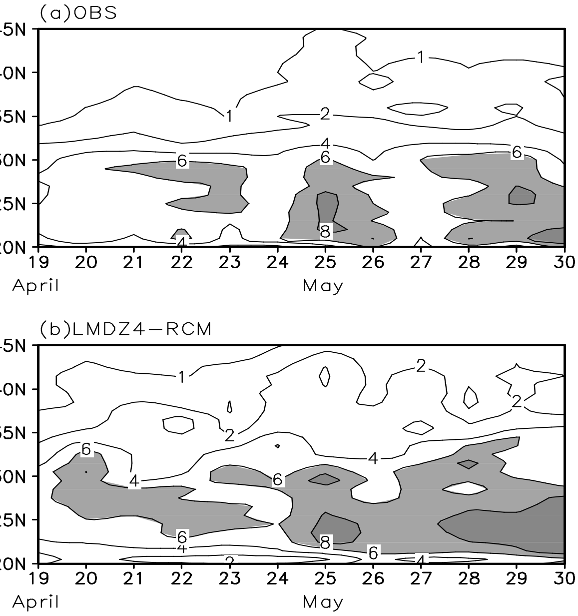

Fig. 4. Time (pentad)-latitude Hovmöller diagrams showing the 107°–122°E averaged precipitation (mm d^{-1}) from April to May for (a) station observation and (b) model simulation averaged during 1990–1999.

(to the north of 35°N), the precipitation increases abruptly in early May, which is also captured by the model. But the simulated rainfall in North China is generally larger than the observed. This deficiency may be partially attributed to the model's biases in reproducing the atmospheric circulation. As can be seen in Fig. 3, the model overestimates the strength of the low-level southerly over southeastern China, indicating more water vapor being transported to the mainland of China from the ocean. On the other hand, the model generates stronger northerlies in North China. This implies that there are stronger interactions between the mid-latitude and the subtropics in the simulation, which also favors for excessive precipitation in North China.

Through the above comparisons, the LMDZ4-RCM is demonstrated to be capable of reproducing main circulation systems in East Asia and the distribution of the precipitation in East China. Then the model will be used in the following to investigate the physical mechanism of the late spring drought in Southeast China.

3. Mechanism of the late spring drought

3.1 *Impact of large-scale circulation changes*

With the LMDZ4-RCM validated, a first control experiment is performed to reproduce the inter-

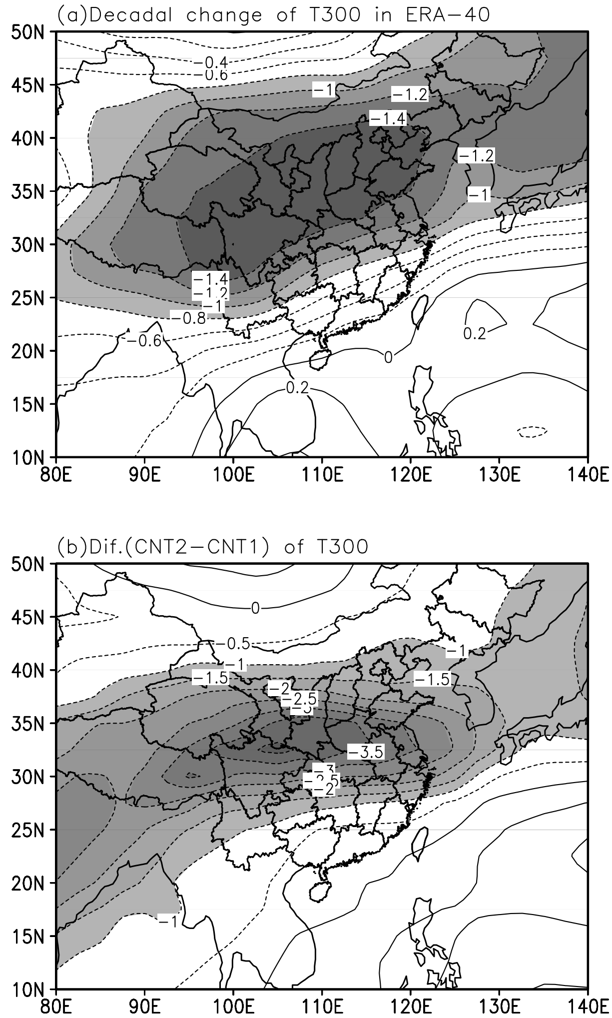

Fig. 5. Late spring temperature changes at 300 hPa (a) in ERA-40 (1981–2000 minus 1958–1977), and (b) in the control experiment (CNT2 minus CNT1). The shading in (a) represents changes of the temperature lower than −0.8°C. The shading in (b) represents changes of the temperature lower than −1.5°C.

decadal changes of late-spring atmospheric circulation related to the drought in Southeast China. Our experimental protocol is a simplified one, since the lateral boundary conditions entering into the LMDZ4-RCM are averaged across different years from March to May for the two periods (1981–2000 and 1958–1977, chosen as in Xin et al., 2006). This permits us to easily conduct further sensitivity experiments and to isolate the contribution of the inter-decadal variations in the large-scale mean circulation. A recent verification using the realistic 6-hour-interval lateral boundary forcing from 1958 to 2000 shows similar results for both the mean climate and the inter-decadal variation (Xin, 2007).

Table 1. Configuration of the control experiment and the sensitivity experiment.

	Control experiment		Sensitivity experiment	
	CNT1	CNT2	SNT1	SNT2
Lateral boundary conditions	1958–1977 averaged fields	1981–2000 averaged fields	1958–1977 averaged fields	1958–1977 averaged fields
Temperature in the middle-upper troposphere (about 750–200 hPa)	No constraint	No constraint	Restoration to CNT1	Restoration to CNT2

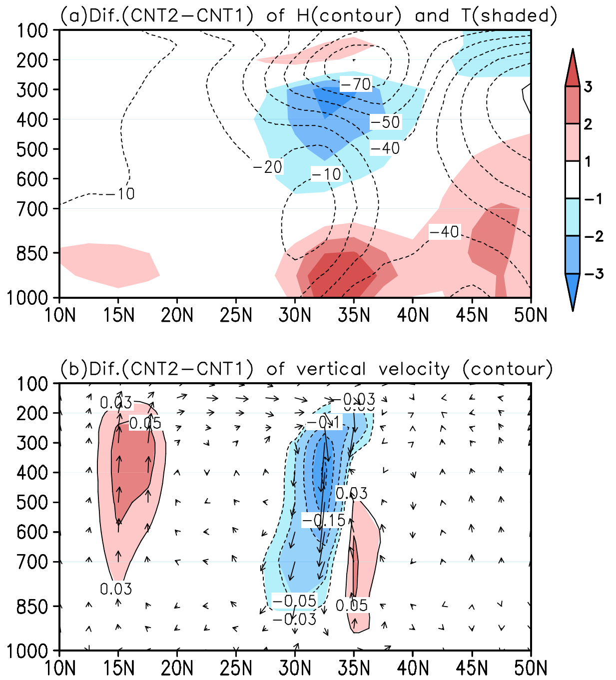

Fig. 6. Latitude-height (pressure, hPa) cross sections along the longitudes from 110°–125°E showing the atmospheric changes in late spring simulated in the control experiment (CNT2 minus CNT1). The upper panel shows the temperature (shaded, °C) and geopotential height (contour, gpm). The lower panel shows the vertical velocity (contour and shaded, m s^{-1}) and wind vectors composed of vertical velocity and meridional wind.

As shown in Table 1, the control experiment consists of two runs, referred to as CNT1 and CNT2, with the averaged large-scale forcing during 1958–1977 and 1981–2000, respectively. Both runs are initiated from a state of 1 March and integrated for three months. Differences of the simulations between CNT2 and CNT1 are considered as the results of the control experiment, designed to show whether the inter-decadal climate changes in East Asia could be reproduced by the model through the forcing in large-scale mean circulation variation.

Inter-decadal changes of the late-spring 300-hPa temperature for both observation and simulation are shown in Fig. 5. We can see that the observed inter-decadal cooling over central China is captured by the model, though with a stronger intensity. The simulated cooling extends from west to east in central China, while the observed cooling center is tilted from Southwest China to Northeast China spanning over a broader region. Such discrepancy between the observation and the simulation can be partly attributed to the experimental design of the control experiment, which employs mean atmospheric fields as lateral boundary forcing, without taking into account any atmospheric transient eddies. The latter can be important for the realism of the model simulations. These biases do not affect our further exploration, since we mainly focus on the climate effects of the upper tropospheric cooling.

The vertical cross section along the longitudes 110°–125°E reveals that the simulated late-spring cooling is prominent in the upper troposphere, with the maximum centered at 300 hPa (Fig. 6a). This is in agreement with the vertical distribution of the observed inter-decadal cooling (Fig. 4a in Xin et al., 2006). The cyclonic anomaly over the cooling region in the upper troposphere also agrees well with the observed inter-decadal change (Fig. 6a).

Figure 6b shows that the air descends from the upper troposphere where the cooling exists. The descending air flows southward in the lower troposphere and then rises in the latitudes 13°–18°N, which finally goes back and compensates the sinking air in the upper troposphere. Thus, the anomalous meridional cell is reproduced in the control experiment. As indicated in Xin et al. (2006), the anomalous meridional cell is closely related to the rainfall anomaly. The descending motions suppress the convective activity, while the anomalous low-level northerlies reduce the water vapor being transported to China. Thus the precipitation decreases in the region 28°–33°N, 108°–128°E, covering the southeastern part of the upper-cooling region (Fig. 7). It should be noted that the simulated inter-decadal dry zone locates slightly to the north of the observed one, which is in the latitudes of 26°–31°N (Fig. 1b in Xin et al., 2006). This may be attributed to the bias of the model's precipitation climatology itself which has a small northward shift (Figs. 3 and 4).

In summary, by using observed large-scale mean

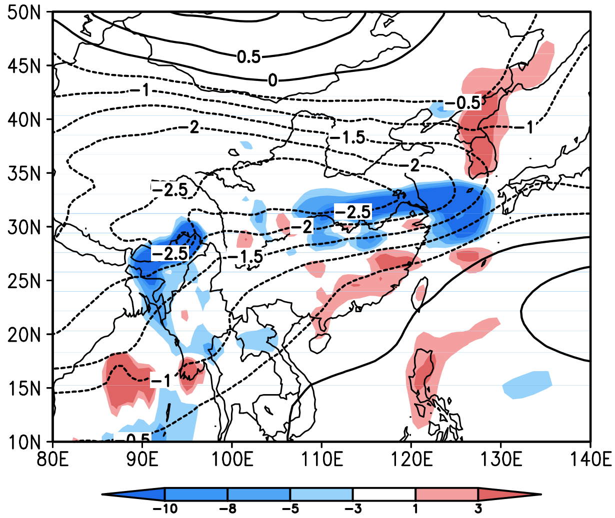

Fig. 7. Changes of the upper tropospheric temperature (500–250 hPa) (contour, °C) and the precipitation (shaded, mm d^{-1}) in late spring simulated in the control experiment (CNT2 minus CNT1).

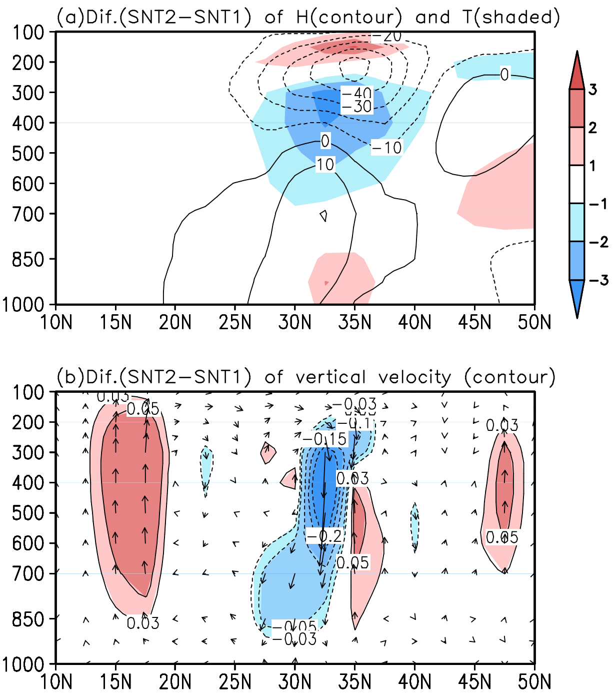

Fig. 8. Same as in Fig. 6, but from the sensitivity experiment (SNT2 minus SNT1).

atmospheric fields as lateral boundary conditions in LMDZ4-RCM, we can reproduce successfully the major characteristics of climate variations in East Asia during the past half century. They include a cooling in the upper troposphere, an anomalous meridional overturning cell, and the associated rainfall decrease located in the southeastern of the upper tropospheric cooling region. Therefore, changes in large-scale mean atmospheric circulation seem to be responsible for the drought occurred in East China. We have carried out similar experiments with different initial states (not shown), which confirm the above results.

3.2 *Role of the upper tropospheric cooling*

The upper tropospheric cooling was considered as a main ingredient in Xin et al. (2006) for the late-spring drought in Southeast China, although we do not know precisely how it is induced by the large-scale boundary forcing, neither any feedback between this upper tropospheric cooling and the precipitation anomalies. We will take a further step toward understanding its role through a sensitivity experiment with the LMDZ4-RCM. The sensitivity experiment includes two runs (SNT1 and SNT2). They share the same initial state and lateral boundary conditions as those in CNT1, but the simulated temperature in the middle-upper troposphere (about 750 hPa–200 hPa) of SNT1 and SNT2 are restored to those of CNT1 and CNT2, respectively (Table 1). Through this procedure, the upper-level cooling simulated in the control experiment is imposed in the sensitivity experiment (Fig. 8a). The simulated differences between SNT2 and SNT1 can be considered as responses to the upper tropospheric cooling, which serve as the results of the sensitivity experiment. The contribution of the upper tropospheric cooling to the drought can thus be quantified.

As shown in Fig. 8a, in response to the imposed upper-level cooling, cyclonic anomalies and anticyclonic anomalies are generated, respectively, above and below the cooling center, as expected from the thermal wind relationship. The upper-level cyclonic and low-level anticyclonic anomalies imply, in the southeast flank of the cooling region, anomalous southerlies in the upper troposphere and northerlies in the lower troposphere (Fig. 8b). Moreover, the cool air descends from the upper troposphere and thus provokes an anomalous meridional cell. The meridional cell bears remarkable resemblance with that in the control experiment (Fig. 6b). This implies that the occurrence of anomalous meridional circulation could be attributed to the cooling in the upper troposphere.

Since the anomalous meridional cell exerts dominant influences on the rainfall, it is anticipated that the rainfall anomaly in the sensitivity experiment bears similar characteristics to that in the control experiment. This is verified in Fig. 9, which shows that the precipitation decreases in the southeast of the upper cooling region. Such a configuration of the drought and the upper-level cooling agrees well with that in

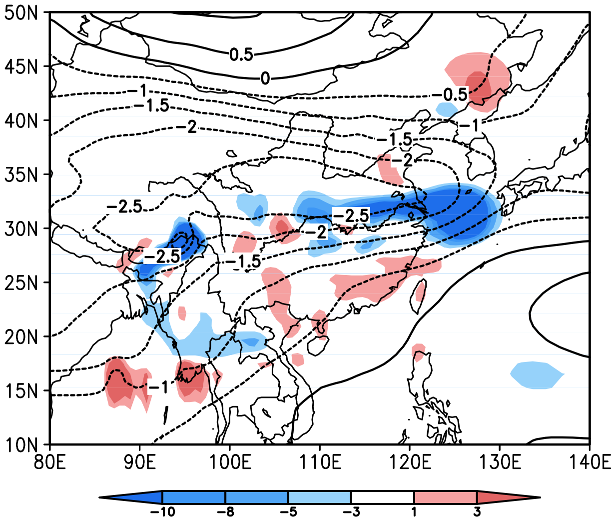

Fig. 9. Same as in Fig. 7, but from the sensitivity experiment (SNT2 minus SNT1).

the control experiment (Fig. 7). This confirms that the upper-level cooling plays an essential role in the formation of the anomalous meridional cell, and consequently the drought to the southeast of the cooling center. These results provide a numerical demonstration to the hypothesis of Xin et al. (2006) that the inter-decadal drought over Southeast China in late spring should be caused by the cooling in the upper troposphere in the past half century.

Although we have shown that the late spring drought in Southeast China could result from East Asian upper tropospheric cooling, the cause of the cooling remains elusive. Some recent studies suggested that this cooling may be related to the inter-decadal change of winter NAO (Yu and Zhou, 2004; Li et al., 2005; Xin et al., 2006). A detailed discussion on the mechanism governing the upper tropospheric cooling is beyond the scope of the present paper and remains to be an open problem demanding further studies.

4. Conclusions

A regional climate model LMDZ4-RCM was used to study the regional climate behavior in spring over East Asia. Its performance in this regard was evaluated with integrations carried out from March to May during each year of 1990 to 1999. Results show that the model reproduces the main features of the 10-yr mean atmospheric circulation over East Asia in AM, including the upper-level jet stream, the East Asian trough and the low-level southerlies over southern China. Spatial distribution and seasonal evolution of AM precipitation in East China are also captured by the model. But in a general manner, the simulated rainfall in North China is larger than the observed, due to partly a stronger low-level convergence in the simulation.

After a general validation of the model LMDZ4-RCM, two experiments were performed to assess the mechanism linking the upper tropospheric cooling with the inter-decadal decrease of the rainfall observed in Southeast China in late spring. The control experiment consists of two runs (CNT1 and CNT2), which used the mean atmospheric circulation of two separate periods of 1958–1977 and 1981–2000 as lateral-boundary conditions. Another sensitivity experiment was carried out with two runs (SNT1 and SNT2) bearing identical lateral boundary conditions but different restoring terms. Through the restoring procedure, the upper-level atmospheric temperature of SNT1 and SNT2 are restored to that of CNT1 and CNT2, respectively. The following conclusions can be drawn through analysis of the two experiments:

(1) Changes of large-scale mean atmospheric circulation during the past half century can induce and explain the main regional circulation changes observed in East Asia in late spring. The regional circulation changes are found to be responsible for the rainfall decrease in Southeast China. We need to mention that similar results were also obtained with another regional climate model RegCM3 (Pal et al., 2007), developed at the International Centre for Theoretical Physics, when it is run in the configuration of our present study. The results are not shown here. This increases the confidence in our results.

(2) Main characteristics of the regional climate change in East Asia can be obtained through restoring the upper troposphere to a cold state in the simulation. It is confirmed that upper tropospheric cooling in East Asia is a causal factor important for the drought in the southeastern of the upper cooling region, although we do not know precisely how it is formed. This conclusion is in agreement with the hypothesis formulated in Xin et al., 2006) through an analysis of the observation data.

Finally, it should be pointed out that, due to the particular experimental design which employs the mean atmospheric fields as lateral-boundary forcing, we did not take into account the effects of atmospheric transient eddies which may play a certain role in our studied phenomenon. This is an issue that we will pursue in the future.

Acknowledgements. This work was jointly supported by the Major State Basic Research Development Program of China (973 Program) under Grant No. 2006CB403603, the Chinese Academy of Sciences International Partnership Creative Group entitled "The Climate System Model Development and Application Studies", China Meteorological Administration under Grant Nos. GYHY200706010 and CCSF2007-32, and the Sino-French PRA program.

REFERENCES

de Rosnay, P., J. Polcher, M. Bruen, and K. Laval, 2002: Impact of a physically based soil water flow and soil-plant interaction representation for modeling large scale land surface processes. *J. Geophys. Res.*, **107**, 10.1029/2001JD000634.

Emanuel, K. A., 1993: A cumulus representation based on the episodic mixing model: The importance of mixing and microphysics in predicting humidity. *Meteor. Monogr.*, **24**, 185–192.

Fouquart, Y., and B. Bonnel, 1980: Computations of solar heating of the Earth's atmosphere: A new parametrization. *Contrib. Atmos. Phys.*, **53**, 35–62.

Genthon, C., G. Krinner, and E. Cosme, 2002: Free and laterally-nudged Antarctic climate of an Atmospheric General Circulation Model. *Mon. Wea. Rev.*, **130**, 1601–1616.

Hourdin, F., and Coauthors, 2006: The LMDZ4 general circulation model: Climate performance and sensitivity to parametrized physics with emphasis on tropical convection. *Climate Dyn.*, doi:10.1007/s00382-006-0158-0.

Hu, Z-Z., Y. Song, and R. G. Wu, 2003: Long-term climate variations in China and global warming signals. *J. Geophys. Res.*, **108**(D19), 4614, doi:10.1029/2003JD003651.

IPCC, 2007: *Climate Change 2007: The Physical Science Basis. Contribution of Working Group I to the Fourth Assessment Report of the Intergovernmental Panel on Climate Change*. Solomon et al., eds., Cambridge University Press, Cambridge, United Kingdom and New York, NY, USA, 996pp.

Krinner, G., and C. Genthon, 1998: GCM simulations of the Last Glacial Maximum surface climate of Greenland and Antarctica. *Climate Dyn.*, **14**, 741–758.

Krinner, G., and Coauthors, 2005: A dynamic global vegetation model for studies of the coupled atmosphere-biosphere system. *Global Biogeochemical Cycles*, **19**, GB1015, doi:10.1029/2003GB002199.

Le Treut, H., Z. X. Li, and M. Forichon, 1994: Sensitivity study of the LMD GCM to greenhouse forcing associated with two different cloud water parametrizations. *J. Climate*, **7**, 1827–1841.

Li, J., R. C. Yu, T. J. Zhou, and B. Wang, 2005: Why is there an early spring cooling shift downstream of the Tibetan Plateau? *J. Climate*, **18**, 4660–4668.

Li, Z. X., 1999: Ensemble atmospheric GCM simulation of climate interannual variability from 1979 to 1994. *J. Climate*, **12**, 986–1001.

Menendez, C. G., A. C. Saulo, and Z. X. Li, 2001: Simulation of South American wintertime climate with a nesting system. *Climate Dyn.*, **17**, 219–237.

Morcrette, J. J., L. Smith, and Y. Fouquart, 1986: Pressure and temperature dependence of the absorption in longwave radiation parametrizations. *Contrib. Atmos. Phys.*, **59**, 455–469.

Pal, J. S., and Coauthors, 2007: Regional Climate Modeling for the Developing World: The ICTP RegCM3 and RegCNET. *Bull. Amer. Meteor. Soc.*, **88**, 1395–1409.

Sadourny, R., and K. Laval, 1984: January and July performance of the LMD general circulation model. *New Perspectives in Climate Modeling*, A. Berger, and C. Nicolis, Eds., Elsevier, Amsterdam, 173–197.

Uppala, S. M., and Coauthors, 2005: The ERA-40 re-analysis. *Quart. J. Roy. Meteor. Soc.*, **131**, 2961–3012, doi:10.1256/qj.04.176.

Xin, X. G., R. C. Yu, T. J. Zhou, and B. Wang, 2006: Drought in late spring of South China in recent decades. *J. Climate*, **19**, 3197–3206.

Xin, X. G., 2007: Observational analysis and numerical simulation of the decadal change in late spring climate over East China in the last four decades. Ph. D. dissertion, Institute of Atmospheric Physics, Chinese Academy of Sciences, 84pp. (in Chinese)

Yang, F. L., and K-M. Lau, 2004: Trend and variability of China precipitation in spring and summer. *International Journal of Climatology*, **24**, 1625–1644.

Yu, R. C., and T. J. Zhou, 2004: Impacts of winter-NAO on March cooling trends over subtropical Eurasia continent in the recent half century. *Geophys. Res. Lett.*, **31**, L12204, doi:10.1029/2004GL019814.

Yu, R. C., B. Wang, and T. J. Zhou, 2004: Tropospheric cooling and summer monsoon weakening trend over East Asia. *Geophys. Res. Lett.*, **31**, L22212, doi: 10.1029/2004GL021270.

Zhai, P. M., X. B. Zhang, H. Wang, and X. H. Pan, 2005: Trends in total precipitation and frequency of daily precipitation extremes over China. *J. Climate*, **18**, 1069–1108.

Zhou, T. J., and Z. X. Li, 2002: Simulation of the East Asian summer monsoon using a variable resolution atmospheric GCM. *Climate Dyn.*, **19**, 167–180.